

Notes

Temperature Dependence of the Intramolecular Disorder in the High-Temperature Phase of Poly(tetrafluoroethylene) (Phase I)

C. DE ROSA, G. GUERRA, V. PETRACONE,*
R. CENTORÉ, and P. CORRADINI

*Dipartimento di Chimica, Università di Napoli,
Via Mezzocannone 4, 80134 Napoli, Italy.
Received July 28, 1987*

Introduction

The crystal transformations and molecular disorder introduced into poly(tetrafluoroethylene) (PTFE) through the two solid-solid transitions at 19 and 30 °C have been widely investigated by X-ray diffraction.¹⁻⁸ There is a long-range order in the periodic placement of the chain axes at any temperature. However, different types and amounts of intermolecular and intramolecular disorder are involved at different temperatures.

The types of intermolecular disorder have been substantially clarified. A short-range order (<50 Å) involving the positioning of the fluorine atoms of neighboring helices at nearly the same height is present in both phase IV (stable between 19 and 30 °C) and phase I.⁸ However, in phase I, small translational displacements along *c* around the average values would be allowed at low temperatures,⁸ and any residual translational order would be lost at higher temperatures.⁶ Alternating rows of right- and left-handed helices would be present in phase IV but absent in phase I.⁷⁻⁹ Small angular displacements of the helices along *c* with respect to an ordered structure would be present in phase IV while a completely random angular arrangement is present in phase I.²

Some intramolecular disorder is also present in phase I and increases with temperature. In fact, the two intense halos on the seventh and eighth layer lines, typical of the 15/7 helical conformation, approach each other with increasing temperature and finally form a single layer line.⁵

The hypothesis that the intramolecular disorder corresponds to helix reversals has been supported in several studies^{4,6,8,10} and can account for the collapse of the two layer lines into a single layer line.^{4,5} In addition, calculations of Fourier transforms for bundles of helices suggest that increasing the number of helix reversals should increasingly narrow the profile of the single layer line.⁸ On the basis of the reasonable assumption that the number of helix reversals increases with temperature, this narrowing of the line profile with temperature is to be expected.

In order to verify this expectation, we have determined X-ray diffraction patterns for the region corresponding to the seventh and eighth layer lines over the temperature range 20–160 °C. We have also compared these patterns with calculations of Fourier transforms of bundles of parallel chain molecules and have estimated the average number of helix reversals at different temperatures.

Experimental Section

The PTFE fibers were supplied by Montefluos S.p.A. The X-ray diffraction patterns were obtained with Ni-filtered Cu K α radiation. Fiber patterns were obtained with a cylindrical camera with a temperature control of ± 3 °C, and intensity measurements were made with a microphotometer along curves corresponding to fixed ξ values. Powder patterns were obtained with an auto-

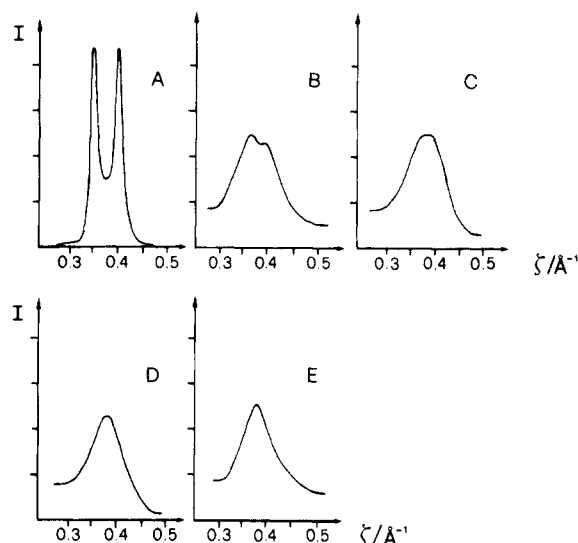


Figure 1. X-ray diffraction patterns of fibers of PTFE at $\xi = 0.20$ Å⁻¹ in the region of seventh and eighth layer lines as a function of the reciprocal lattice coordinate ξ : (A) 21 °C; (B) 40 °C; (C) 60 °C; (D) 100 °C; (E) 160 °C.

matic Philips powder diffractometer with a temperature control of ± 0.5 °C.

Fourier transforms were calculated by the method described by us,¹¹ which has been used for study of the disordered phases of PTFE.⁸ A thermal factor with anisotropic parameters ($B_x = 10$ Å² and $B_z = 5$ Å²) was assumed.^{8,11}

The calculations were performed on pseudohexagonal bundles of 19 parallel chains of PTFE in a completely random angular arrangement, with a constant distance between the axes of adjacent chains (5.66 Å). In models without helix reversals, right- and left-handed helices, having a 15/7 symmetry, are randomly distributed. The helix reversals were obtained by inserting at least one bond in the trans conformation.⁴

Since the reported calculations are for a fixed value of ξ , the lateral size of the bundle does not affect the results significantly. However, Fourier transform calculations for a bundle rather than for an isolated chain are helpful in providing a direct average between situations with different reversal locations. For each case a further average of the results for seven different bundles was performed.

The length of the chains, for sufficiently high values does not strongly influence the calculated patterns. The value chosen was 130 Å (chains formed by 100 CF₂ groups), which is similar to the average coherent length derived from the broadness of the (0,0,15) reflection at 175 °C.⁶

Results

X-ray Diffraction Patterns. The line profiles of the fiber patterns along the reciprocal coordinate ξ , at $\xi = 0.20$ Å⁻¹, at temperatures in the range 20–160 °C are shown in Figure 1.

Below the 30 °C transition the seventh and eighth layer lines (at $\xi = 0.359$ and 0.410 Å⁻¹, respectively) are well defined (Figure 1A). As previously described,⁵ with increasing temperature the two layer lines become ill defined and approach each other (Figure 1B) and finally merge to a single broad layer line centered at $\xi = 0.385$ Å⁻¹ (Figure 1C). With further increase in temperature, the profile of the single layer line becomes increasingly narrow, at least up to 160 °C (Figure 1D,E).

This behavior is also seen in the powder patterns in the 2θ range 30–50° (Figure 2). In all the patterns of Figure

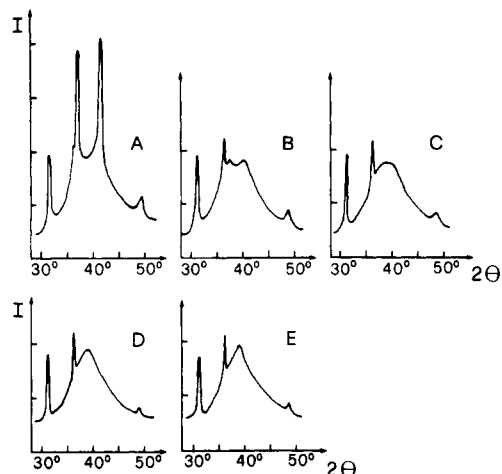


Figure 2. X-ray diffraction powder patterns of PTFE: (A) 21 °C; (B) 35 °C; (C) 50 °C; (D) 100 °C; (E) 160 °C.

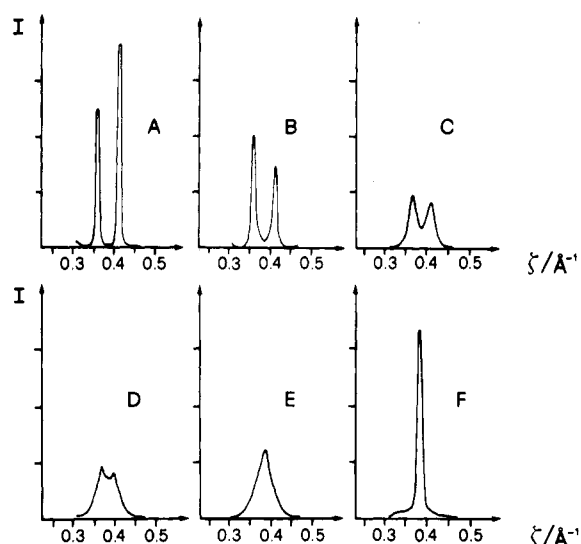


Figure 3. Calculated X-ray diffraction profiles at $\xi = 0.205 \text{ \AA}^{-1}$ as a function of ζ ; (A) model with no reversal of the handedness of the helices; (B–F) models with one reversal of the handedness of the helices every 50 CF_2 groups (B), 20 CF_2 groups (C), 13 CF_2 groups (D), 10 CF_2 groups (E), and 5 CF_2 groups (F).

2 there are equatorial diffraction peaks at $2\theta = 31.6^\circ$, 36.8° , and 49.3° . Below 30°C , the diffraction peaks of the seventh and eighth layer lines at $2\theta = 37^\circ$ and 41.6° are also present. Above 30°C , while the nonequatorial Bragg reflections disappear, the halos corresponding to the two layer lines are still present and approach each other as the temperature increases. At 50°C there is only a single halo, which becomes sharper with increasing temperature.

Fourier Transform Calculations. Calculated profiles for bundles of chains along ζ , at $\xi = 0.205 \text{ \AA}^{-1}$, are shown in Figures 3 and 4. The pattern in Figure 3A corresponds to the assumed model with no reversals of the handedness of the helices. The patterns in Figure 3B–F correspond to models with one reversal (on average) every 50, 20, 13, 10, and 5 CF_2 groups. The peaks in Figure 3A do not correspond to Bragg reflections. In fact, the completely random angular arrangement of the parallel chains generates broad halos along ξ .^{2,8} On increasing the average number of reversals, the two layer lines approach each other, and a sharp single layer line is obtained for one reversal on average every 10 atoms. Further increases in the number of helix reversals make the layer line sharper.

Since a 2/1 helix (all trans conformations for the backbone dihedral angles) has to give a single layer line

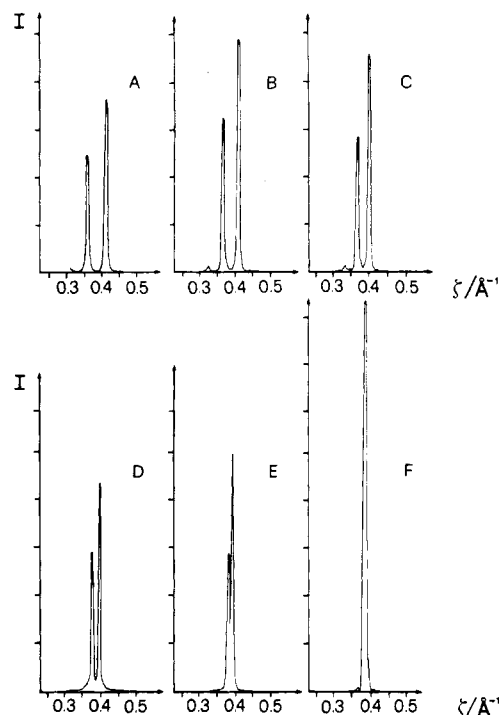


Figure 4. Calculated X-ray diffraction profiles at $\xi = 0.205 \text{ \AA}^{-1}$ as a function of ζ for a model with no helix reversals and in which there are a fraction of backbone dihedral angles in the *trans* conformation equal to (A) 0%, (B) 20%, (C) 40%, (D) 60%, (E) 80%, and (F) 100%.

at $\xi = 0.385 \text{ \AA}^{-1}$, the influence of trans conformations on the Fourier transforms in the absence of helix reversals was also investigated. The calculated patterns of Figure 4A–F refer to models in which the fraction of backbone dihedral angles in the *trans* conformation (randomly distributed) is equal to 0, 20, 40, 60, 80, and 100%, respectively. There are two well-defined layer lines which approach each other as the fraction of trans conformations increases and collapse to a single layer line at 100% trans conformations.

Discussion

Comparison of the experimental (Figures 1 and 2) and calculated (Figure 3) patterns indicates that the temperature dependence of the X-ray diffraction pattern in the region of the seventh and eighth layer lines is in agreement with the hypothesis that the number of helix reversals in phase I increases with temperature. The calculated line profiles above room temperature are considerably sharper than the experimental profiles, due to the simplifying assumption of perfect helical stretches, which is increasingly unrealistic with increasing numbers of helix reversals. More realistic models should include some irregularities in the conformation of the helical stretches, besides the inversions, which would produce broader line profiles.

The calculations of Figure 4 suggest that intramolecular defects which do not involve inversions cannot account for the collapse of the two layer lines of the experimental patterns. The Fourier transform calculations of Figure 3 indicate instead that even small variations in the number of reversals can account for dramatic changes in the experimental patterns. In the framework of our assumptions, the calculated patterns for the models with one reversal every 20 and 10 CF_2 groups could roughly account for the experimental patterns of phase I, for the lowest and highest temperatures, respectively.

The variation in the population of the defects (p) with temperature, suggested by the present calculations, is in

qualitative agreement with substantial temperature independence of the energy per defect ($E = -RT \ln p$).

Acknowledgment. Financial support of Montefluos S.p.A., of the National Research Council (C.N.R.), and of the Ministry of Public Education (Italy) is gratefully acknowledged.

Registry No. PTFE, 9002-84-0.

References and Notes

- (1) Bunn, C. W.; Howells, E. R. *Nature (London)* **1954**, *174*, 549.
- (2) Clark, E. S.; Muus, L. T. *Z. Kristallogr.* **1962**, *117*, 119.
- (3) Muus, L. T.; Clark, E. S. *Polym. Prepr. (Am. Chem. Soc., Div. Polym. Chem.)* **1964**, *5*, 17.
- (4) Corradini, P.; Guerra, G. *Macromolecules* **1977**, *10*, 1410.
- (5) Matsushige, K.; Enoshita, R.; Ide, T.; Yamauchi, N.; Taki, S.; Takemura, T. *Jpn. J. Appl. Phys.* **1977**, *16*, 681.
- (6) Yamamoto, T.; Hara, T. *Polymer* **1982**, *23*, 521.
- (7) Yamamoto, T.; Hara, T. *Polymer* **1986**, *27*, 986.
- (8) Corradini, P.; De Rosa, C.; Guerra, G.; Petraccone, V. *Macromolecules* **1987**, *20*, 3043.
- (9) Farmer, B. L.; Eby, R. K. *Polymer* **1985**, *26*, 1944.
- (10) De Santis, P.; Giglio, E.; Liquori, A. M.; Ripamonti, A. *J. Polym. Sci., Part A* **1963**, *1*, 1383.
- (11) Corradini, P.; Petraccone, V.; De Rosa, C.; Guerra, G. *Macromolecules* **1986**, *19*, 2699.

Hydrodynamic Radius of Polystyrene in *n*-Butyl Chloride

Y. F. MAA and S. H. CHEN*

Department of Chemical Engineering, University of Rochester, Rochester, New York 14627.

Received July 30, 1987;

Revised Manuscript Received September 2, 1987

Introduction

The conformational dynamics of an isolated macromolecule in solution can be revealed through intrinsic viscosity or translational diffusivity measurements. The macromolecular dimension obtained from transport properties has frequently been interpreted in terms of the chain statistics and the excluded volume and solvent effects, together with the static dimension (e.g., the radius of gyration R_g) derived from light or neutron scattering experiments. For instance, the ratio R_g/R_h was believed to assume a universal value under Θ conditions.^{1,2} However, both Fixman³ and Cherayil et al.⁴ have questioned such universality. The failure of the universality might have arisen from the fact that both the excluded volume and solvent perturbations give rise to different quantitative effects on R_h and R_g . Hence, it is important that solvent effects on unperturbed dimensions be clearly understood before the excluded volume effects can possibly be correctly interpreted.

In the present study the translational diffusion coefficients have been determined with the extended Taylor dispersion technique⁵ for a series of polystyrene standards with peak molecular weight M from 503 to 10^5 g/mol in cyclohexane at the Θ temperature of 308 K and in *n*-butyl chloride (a good solvent) at temperatures from 278 to 348 K. The hydrodynamic radii R_h calculated from the measured values of translational diffusion coefficients in *n*-

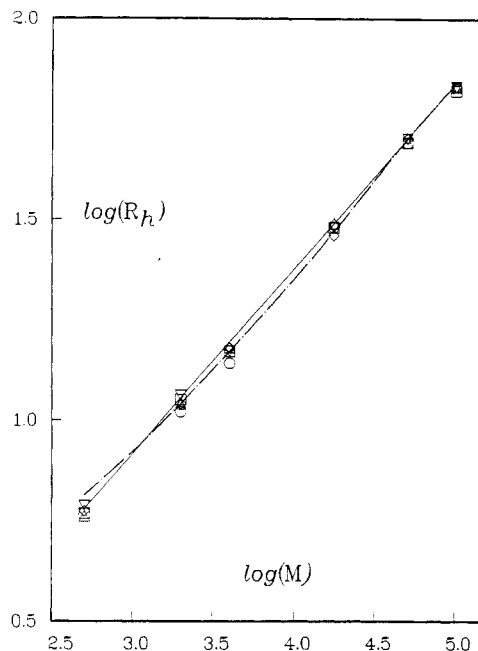


Figure 1. R_h as a function of M . Symbols representing experimentally determined values: (○) at 308 K in cyclohexane; (□) 278 K, (Δ) 298 K, (◇) 323 K, and (▽) 348 K all in *n*-butyl chloride. Solid line for R_h versus M^0 relationship; dot-dash curve for wormlike chain model prediction.

Table I
Characteristics of Polystyrene Standards from Pressure Chemical

M	M_w/M_n	notation	M	M_w/M_n	notation
503	≤1.03	PS0.5K	17 500	≤1.06	PS17.5K
2000	≤1.06	PS2K	50 000	≤1.06	PS50K
4000	≤1.06	PS4K	100 000	≤1.06	PS100K

butyl chloride will be compared with those in cyclohexane at Θ temperature to examine possible solvent effects. This comparison should furnish new insights into the roles played by phenyl group/solvent interaction and solvent molecular geometry (acyclic versus cyclic) in affecting polystyrene molecular conformation. Both factors have been cited^{6,7} to interpret the solvent effects on intrinsic viscosity of polystyrene in a variety of solvents.

Experimental Section

The basis of determining the translational diffusion coefficient of a polymer solute at infinitely dilute solution was presented previously.⁵ Note that the dispersion technique results in the diffusivity corresponding to the most probable molecular weight M and that for a nearly monodisperse polymer standard with $M_w/M_n \leq 1.06$, as was encountered in the present study; the dispersion peak is virtually Gaussian, suggesting that the polystyrene samples as listed in Table I behave like monodisperse solutes. The experimental apparatus and procedures are as described elsewhere.⁵ Solvents cyclohexane (99.0 + %, Aldrich Chemical Co.) and *n*-butyl chloride (99.5 %, Alltech Associates) were both dried over phosphorus pentoxide (99.2 %, J. T. Baker) and then distilled before usage.

Results and Discussion

Summarized in Table II are the translational diffusion coefficients D measured with the extended Taylor dispersion technique⁵ for polystyrene in cyclohexane and

* Author to whom correspondence should be addressed.